

Lasers in Manufacturing Conference 2017

Influencing the ablation efficiency in ultra-short pulse laser micro structuring by using a deformable mirror for beam shaping

Marco Smarra^{a,*}, Klaus Dickmann^a

^a*Laser Center University of Applied Sciences Muenster, Stegerwaldstr. 39, 48565 Steinfurt, Germany*

Abstract

The increasing average laser power and especially the increasing pulse energies of ultra-short pulse laser systems enhance the demand of new processing strategies for an efficient ablation process. Polygon scanners were developed to offer high scanning speeds which are often required in combination with a high pulse repetition rate. An increase of the pulse energy raises the formation of substructures and therefore roughness on ablation ground instead of enhancing the amount of removed material. The optimal laser fluence for material processing can be determined by material properties like the optical penetration depth and the threshold fluence. In this study it is shown that the laser fluence can be optimized by using a beam shaping tool. The tool used in this study is a deformable mirror with 35 individual controllable segments and a closed mirror surface. These type of beam shaping elements are one of the most suitable tools for high power laser applications due to the absence of intensity losses due to diffraction or absorption. The mirror deformation leads to a modulation of the incident wavefront and therefore to a variation of the beam shape in the focal plane. These spot shapes were used for micro structuring of metal sheets. The structured areas were analyzed considering the depth, roughness and edge angles. Based on this information a high precision determination of the ablation efficiency is possible. Finally, these results were used to demonstrate various practical structuring examples successfully.

Keywords: micro processing; ablation; system technology; deformable mirror

* E-mail address: marco.smarra@fh-muenster.de .

1. Introduction

The increasing average powers and the decreasing costs per watt for ultra-short pulse lasers (usp-laser) lead to a growing application field for these laser systems. The well known advantages of the short interaction time between the laser pulse and the material leads to a low thermal influence to the work piece. This offers a precision production tool for the generation of small structures. However, generating small structures leads to a poor removal rate (ablated volume per time) which can be overcome by the use of high power usp-lasers.

Average powers of more than 100 W are industrial available with repetition rates of a few MHz and pulse energies of a few 100 μJ . To use these high average powers in structuring applications, new process strategies have to be developed. Otherwise, the advantages of the short interaction time are prevented due to heat accumulation, which lead to an inefficient process and a higher surface roughness (Hildenhagen et al. 2012). By the knowledge that the average power (P_{av}) is the multiplication of the pulse repetition rate (f_{Rep}) and the pulse energy (E_{Pulse}), developments for new processing strategies are

- High scanning speeds using polygon scanners to reduce the pulse overlap and thereby decrease the thermal influence, (Loor et al. 2014).
- Parallel processing to increase the throughput.

For parallel processing two strategies are possible: At first, the beam can be split into several symmetric beams, e.g. for multi-beam drilling using one scanner to drill symmetric structures (Büsing et al.). Secondly, the beam can be split into parallel working scanning heads, to perform the same process on two or more samples at the same time (Manz AG 2015).

In this study beam shaping as process strategy is analyzed. The ablation process can be described by the logarithmic ablation law. Neuenschwander et. al. have demonstrated that the ablation efficiency – the ablated volume (dV) per time and per average power $dV/(dt \cdot P_{av})$ – depends on the laser fluence (F_0) described by the pulse energy and the beam area (A_{Beam}) (Neuenschwander et al. 2014). This can be extended for a Gaussian beam shape with two perpendicular waist diameter (w_x and w_y) by

$$F_0 = \frac{E_{Pulse}}{A_{Beam}} = \frac{2 \cdot E_{Pulse}}{\pi \cdot w_x \cdot w_y} \quad (1)$$

Furthermore they have shown, that the ablation efficiency depends on material parameters like the optical penetration depth (δ_{op}) and the threshold fluence (F_{th}).

$$\frac{dV}{dt \cdot P_{av}} = \frac{1}{2} \cdot \frac{\delta_{op}}{F_0} \cdot \ln^2 \left(\frac{F_0}{F_{th}} \right) \quad (2)$$

The ablation efficiency shows a maximal removal rate at e^2 times the threshold fluence. Schille et. al. called this section the “mid-fluence-regime”, to indicate the delimitation of lower and higher fluences (Schille et al. 2015). Lauer et. al. demonstrated the efficiency for three different waist diameters on the surface (Lauer et al. 2015).

Influencing the intensity distribution of a laser beam is called beam shaping: The easiest way of beam shaping is the use of a lens to define a desired spot diameter in the focal plane. More complex intensity distributions can be achieved by diffractive optical elements (DOE), which are used to generate Top-Hat beam shapes (Rung 2013). More flexible beam shaping systems can be built by using a spatial light modulator (SLM), which suffer from high intensity losses due to diffraction. Heberle et. al. investigated the use of AOM and EOM for beam shaping (Heberle et al. 2016). Here, due to the crystal size the maximal pulse energy is limited.

In this study, a deformable mirror is used to manipulate the incident laser beam. The influence of the mirror deformation leads in a focus shift, astigmatic or cylindrical lens behavior. This results in a variation of the beam shape on the material surface, e.g. larger beam diameter or elliptical shapes. The concept of the laser system was presented earlier (Smarra et al. 2015). Previous work showed the ablation behavior for astigmatic laser beams (Smarra und Dickmann 2016). In this study, the ablation efficiency and the influence to structuring results by using asymmetric laser beam shapes are shown.

2. Experimental Setup

For the ablation efficiency measurement small cavities with lateral dimensions of $2 \times 2 \text{ mm}^2$ are irradiated by an ultrashort pulse laser (Trumpf TruMicro 5050, $\tau \approx 8 \text{ ps}$, $f_{\text{Rep,max}} = 800 \text{ kHz}$, $E_{\text{p,max}} = 62.5 \text{ }\mu\text{J}$) and a galvo scanner (HurryScan II, Scanlab). The focal length of the f-Theta objective used in the scanning device is 100 mm. The scanning speed is adapted to achieve a constant pulse-to-pulse distance regarding the repetition rate. In this study the pulse-to-pulse distance is kept constant: Using a shaped beam even a variation of the focus position leads to a change in the pulse overlap. This influence is not presented in this study. The ablation time mentioned for the efficiency is the theoretical “laser-on-time”. This means, that by the knowledge of the structured area, the pulse distance and the repetition rate of the laser the “laser-on-time” can be calculated. Due to a variation in the acceleration and deceleration of the galvo mirrors respectively to the scanning speed, there is a difference between the real processing time and the theoretical “laser-on-time”. By using the theoretical time low and high scanning speeds can be compared more sufficiently. In addition, the results of this study can be compared to those performed by a polygon scanner.

The structured surface is analyzed by a topographic sensor (CHROcodile S, Precitec, 3 mm chromatic sensor). By the knowledge of the ablated depth, the ablated volume can be calculated. By scanning the topography of the treated areas, the roughness or edge form of the surface can be investigated. Two usb-microscopes are used to document the pre- and post-processing condition of the surface.

The material used in this study is 2 mm thick stainless steel (1.4301). The outer dimensions of the sample are $70 \times 70 \text{ mm}^2$, which offers a large number of samples structures with a dimension of $2 \times 2 \text{ mm}^2$. To reduce thermal influence between two fields next to each other, the structure areas are fabricated in a randomized order. The surface is cleaned by isopropanol before inserting the sample into the machine and by air before each laser treatment. The last mentioned cleaning step is used to reduce the dust from former structuring processes of nearby test-fields.

For beam shaping a deformable mirror is used in this study (Smarra und Dickmann 2015). This mirror is built by a sandwich structure of a thin piezoelectric ceramic and thin mirror substrate. A piezoelectric ceramic changes its shape when applying an external voltage. The ceramic is divided into 35 individual controllable segments. This offers a high flexibility in the deformation of the ceramic. The mirror combined to the piezoelectric ceramic performs the same deformation as the ceramic. Due to the high reflective coating ($R > 99,99 \% @ 1030 \text{ nm}$) and the closed mirror surface the transmission efficiency is nearly 100 % and no intensity losses due to diffraction occurs. The mirror deformation is controlled by an electric driver, which calculates the voltage for each segment based on a Zernike deformation. The influence of the mirror deformation to the incident beam in the focal plane is investigated by a beam analysis: A CCD-camera captures the intensity profile at various z-positions and a software calculates the beam diameter for circular or elliptical Gaussian intensity distributions. These data can be used to calculate the fluence of the beam.

3. Results

In this section at first the results of manipulating the incident laser beam by the mirror deformation are shown. After that the influence of the beam shape to ablation results are shown. In addition, the influence of the shaped beams to structuring results are demonstrated.

3.1. Beam Analysis

The deformable mirror is used to manipulate the incident laser beam by defocus and astigmatism. A combination of both influences leads to a cylindrical lens behavior with an oval shape on the sample surface. Below the results of the beam analysis are shown.

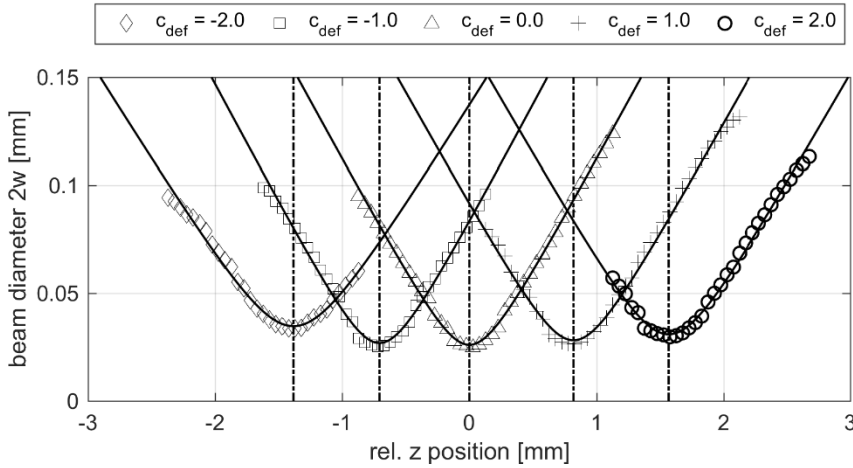


Fig. 1. Beam propagation with varying defocus deformation of the deformable mirror. The waist can be shifted in the range of 3 millimeters. The minimal waist occurs in the nominal focus position.

A defocus deformation of the mirror surface leads to a radial symmetrical influence to the incident beam. The result is a focus shift from the nominal focus position. Fig 1 shows the radial beam diameter in dependence of the relative z-position and the mirror deformation (c_{def}). In the nominal waist position (rel. $z = 0$) the mirror surface is flat and does not influence the incident beam and the focal length of the system is determined by the f-theta lens (in this study 100 mm). The optical system of this setup is designed to perform a linear focus shift. The focus variation also leads to a variation of the waist diameter. The smallest waist diameter can be realized in the nominal focal plane (of the f-theta system).

A further mirror deformation leads to an astigmatic influence to the incident beam. Compared to the focus shift, the waist position can be varied by this deformation. But for an astigmatic deformation there are two perpendicular waists that can be manipulated, Fig. 2 (left). This deformation leads to a linear increase of the distance between the perpendicular waists (Δw), Fig. 2 (right). The distance of the two waists increase linearly, due to the symmetric deformation of the mirror. This is comparable to Fig. 1: Each waist is influenced by a defocus, but in contrary directions - while one axis is focused, the perpendicular axis is defocused. In combination with the scanning optic, the resulting beam propagation is a combination of the two perpendicular axis. The resulting beam shape depends on the relative position of the laser beam to the sample surface: On the one hand, the beam diameter increases in the nominal focus position. On the other hand, the beam shape itself varies when the astigmatic deformation is combined with a focus shift. This influence to the incident beam can be compared to a cylindrical lens.

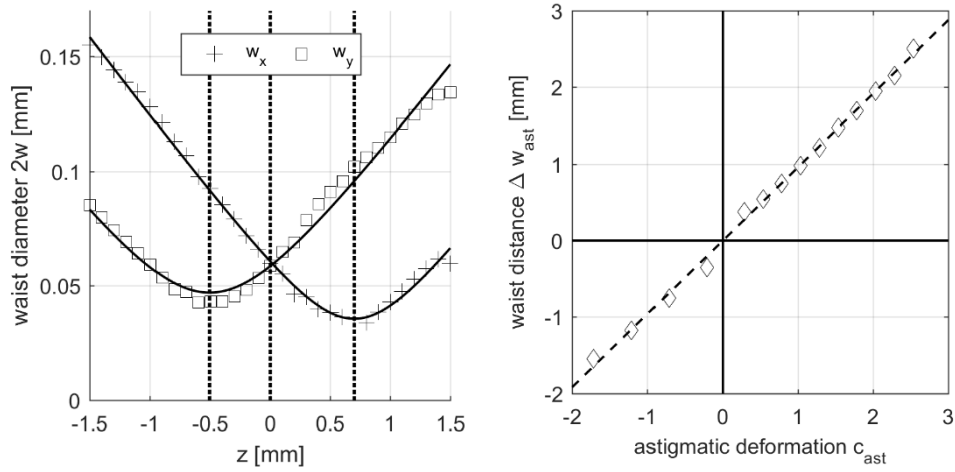


Fig. 2. Influences to incident beam by an astigmatic deformation of the deformable mirror. Left: Beam propagation of the two perpendicular axis. The propagation of each axis equals a Gaussian propagation, but the waist position is shifted contrary from the nominal position. Right: Manipulation of the perpendicular waist distance by the astigmatic deformation of the deformable mirror. Due to the symmetric deformation, the waist distance increase linearly, like the defocus.

3.2. Ablation results

It is shown that the deformable mirror can be used to vary the waist position. By this focus variation the spot diameter of the laser on the sample surface increases. The results of the ablation process using these larger spot diameters are shown in this section.

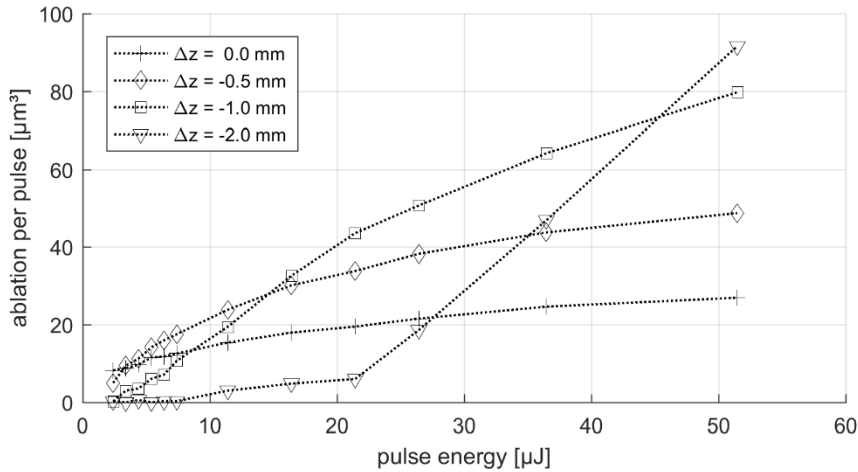


Fig. 3. Ablation per pulse vs. pulse energy for different waist positions: The defocus deformation of the mirror leads to a variation of the focus position of the laser beam. This increases the beam diameter on the sample surface. For low pulse energies, the ablation per pulse is lower the larger the beam diameter on the sample surface is. By increasing the pulse energy, the ablation increases stronger for larger beam diameter: A defocus of -2 mm (waist position in the material) leads to an increase of the ablated volume by a factor of 3 in this setup (f-theta 100 mm). The repetition rate and the pulse-to-pulse distance are kept constantly.

The ablation depth of each $2 \times 2 \text{ mm}^2$ structured area is measured and the ablation per pulse is calculated. In Fig. 3 the ablation per pulse over the pulse energy is shown. The pulse repetition rate and the pulse-to-pulse distance are kept constantly. The waist position is manipulated by the mirror deformation. When the waist of the laser beam is located on the surface, the ablation per pulse follows the logarithmic ablation law. If the waist position of the beam is set below the sample surface into the material the diameter of the laser on the sample surface increases. For a defocus of -1.0 mm the ablation per pulse for low pulse energies is smaller than for the waist position on the sample surface. But for larger pulse energy the ablated volume increases stronger for larger beam areas. This can be seen by comparing the ablation behavior for a defocus of -2.0 mm . The ablation increases strongly after reaching a threshold pulse energy of about $20 \text{ }\mu\text{J}$. The maximum ablation per pulse is more than 3 times higher than for the waist diameter on the sample surface.

The ablation efficiency, the ablated volume per time and average laser power in dependence to the fluence, is shown in Fig. 4. The results are shown for a constant repetition rate and pulse-to-pulse distance. The fluence is varied by the pulse energy. The dependence to the waist position is demonstrated by different markers. After exceeding the threshold fluence, the efficiency increases to a maximum which is about e^2 times the threshold fluence. Further increasing of the laser fluence does not lead to an increase in the ablation efficiency. In fact, the efficiency drops down. The high fluence leads to an increase of the formation of substructures and therefore an increase of the surface roughness. There is a variation in the efficiency depending on the position of the beam waist relative to the sample surface. The quotient of optical penetration depth and laser fluence describe the maximal achievable ablation efficiency. The variation of the maximal ablation efficiency is an indication that the optical penetration depth itself can be influenced by the waist position. The position as

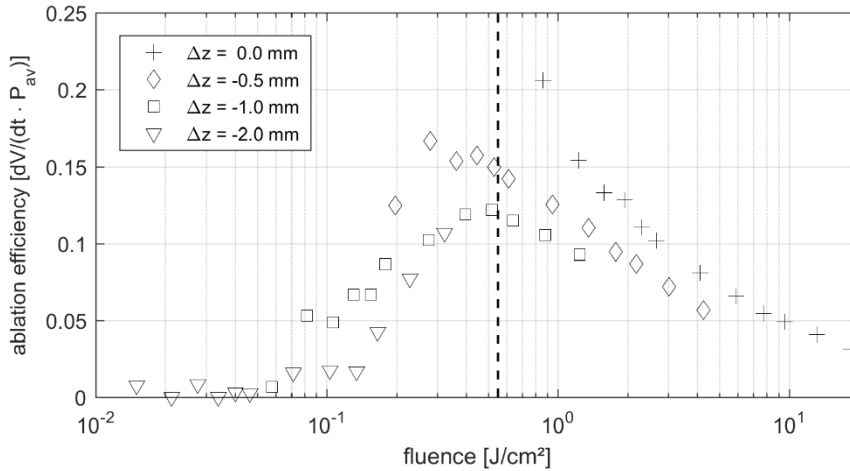


Fig. 4. Ablation efficiency of stainless steel in dependence to the laser fluence on the material surface for different waist positions. The optimal ablation fluence can be achieved by a combination of pulse energy and focus variation using the deformable mirror. The efficiency increases above the threshold fluence to a maximum. After exceeding the maximum, the efficiency drops down. The optimal ablation fluence is determined by $0.5 - 0.6 \text{ J/cm}^2$, depending on the focus position.

The influence of the mirror deformation for astigmatic beam shapes to the ablation per pulse is shown in Fig. 5 on the left side. The pulse energy and the perpendicular waist distance are varied, the repetition rate is kept constantly. The relative beam position is on the sample surface. This means, if the mirror does not influence the beam (flat surface), the perpendicular waists are on the surface of the sample. By influencing the incident beam by an astigmatic deformation the ablation can be increased to a local maximum,

depending on the pulse energy. For a pulse energy of $40 \mu\text{J}$ this is done by factor of 3. The deformation of the mirror surface leads to an optimization of the laser fluence. As seen in the defocus behavior, the optimum of the ablation efficiency depends on material properties like the threshold fluence, Fig. 5, right. By increasing the perpendicular waist distance the beam area increases which leads to a reduction in the fluence. As the fluence is described by ratio of the pulse energy and the beam area for each pulse energy an optimal beam deformation can be realized. On the other hand, for a desired beam shape the optimal pulse energy can be calculated.

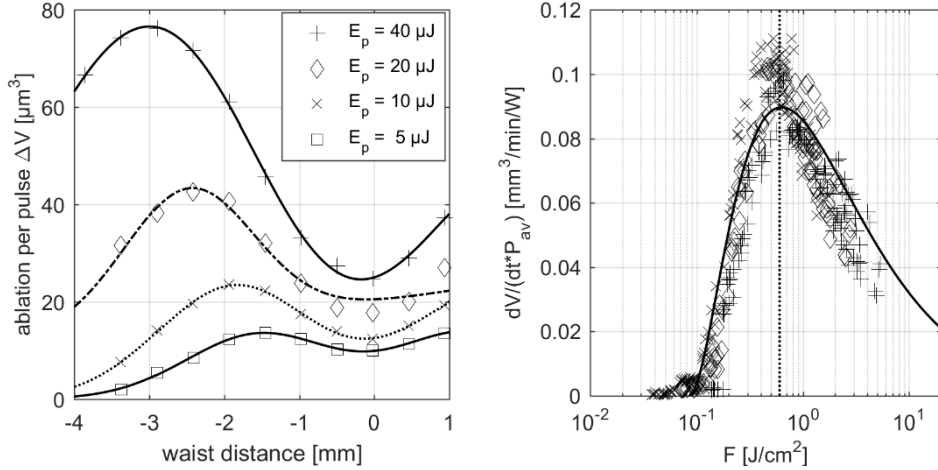


Fig. 5. left: The perpendicular waist distance is increased by an astigmatic deformation of the deformable mirror. The Ablation per pulse in dependence of the perpendicular waist distance is shown. An increase of the waist distance leads to an increase of the beam area. This increase reduces the fluence which can lead to an increase of the ablation per pulse. Right: Ablation efficiency in dependence to the fluence on the sample surface. The maximal ablation efficiency can be achieved for a fluence of $0.6 \text{ J}/\text{cm}^2$, which is comparable to the results for the focus variation.

3.3. Application results for structuring

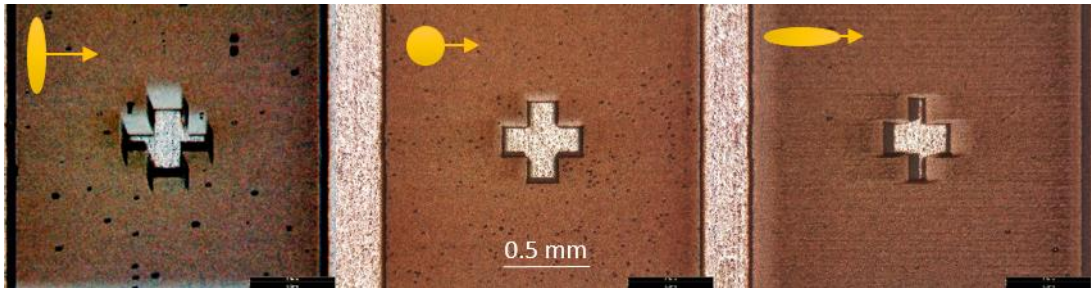


Fig. 6. Influence to the structuring results, using a various orientation of cylindrical (left and right) and astigmatic (middle) beam shapes. In the middle the influence of an astigmatic beam variation is shown. By combining an astigmatic and a focus variation of the incident beam, a cylindrical beam shape results in the focal plane. The orientation of the cylindrical beam is turned by 90° between the left and the right image. The beam shape is indicated top left of each image.

For an efficient ablation process the beam shape can be varied to optimize the ablation fluence, as shown above. In this section, the influence to the structuring results using various astigmatic and cylindrical beam shapes is analyzed. To analyze the influence of the beam shape to the structuring result, a cross contour is

left unstructured in the middle of the laser treated areas. Due to the asymmetric influence of the beam shape, the contour of the structured area changes, as shown in Fig. 6. An astigmatic influence to the laser beam leads to an increase of the beam size in the focal plane. By the combination of an astigmatic influence with a focus shift, the shape of the beam varies. The higher the influence of these beam derivation, the higher is the aspect ratio of the resulting beam shape. This leads to an oval or line-like spot geometry as indicated top left of each microscope picture. The steepness of the edges of the unstructured areas vary due to the slope variation of the intensity profile. It is shown that the orientation of the beam shape can be turned.

4. Conclusion and Outlook

In this study the influence of the beam shape with respect to the ablation efficiency is analyzed. The beam shape is varied by a deformable mirror. The deformable mirror offers a higher transformation efficiency compared to other variable diffractive optics, which is a result of the closed mirror surface. However, its influence is limited due to the small number of controllable segments. For the deformable mirror, the variation of the beam shape in the focal plane can be seen best for defocus and astigmatic mirror deformation. These influences were analyzed due to beam shape and ablation behavior. It can be seen that a variation of the focus leads to a change in the fluence on the work piece. The optimal ablation fluence, which is e^2 times the threshold fluence, can be achieved by choosing a suitable beam shape respectively to the desired pulse energy. The focus variation and the influence of an astigmatic mirror deformation to the incident beam is analyzed. The latter deformation leads to an increase of the perpendicular waist distance of the astigmatic beam, resulting in larger symmetric beam diameter. A comparable ablation efficiency is shown for these beam variation. A combination of astigmatic and defocus mirror deformation leads to a cylindrical beam shape in the focal plane. The influence of this asymmetric beam shape to the structuring results is shown. It can be seen, that the slope of the intensity profile influences the steepness of the resulting structure.

The beam variation by variable beam shaping optics offers a high flexibility in the structuring process. An oval or line-like beam shape could be used for writing isolation channels in electronic devices: By using the large beam diameter perpendicular to the scanning direction, multi passes could be avoided and the scan speed can be reduced to galvo scanning speeds compared to symmetric round spot geometries.

Acknowledgements

The authors thank the Photonics Laboratory of the University of Applied Sciences for providing the deformable mirror and the technical support for the integration into the beam path.

References

- Büsing, L.; Eifel, S.; Loosen, Peter: Design, alignment and applications of optical systems for parallel processing with ultra-short laser pulses, S. 91310. DOI: 10.1117/12.2051614.
- Heberle, Johannes; Bechtold, Peter; Strauß, Johannes; Schmidt, Michael (2016): Electro-optic and acousto-optic laser beam scanners. In: Udo Klotzbach, Kunihiko Washio und Craig B. Arnold (Hg.): SPIE LASE. San Francisco, California, United States, Saturday 13 February 2016: SPIE (SPIE Proceedings), S. 97360.
- Hildenhausen, J.; Engelhardt, U.; Smarra, M.; Dickmann, K. (2012): Material specific effects and limitations during ps-laser generation of micro structures. In: Alexander Heisterkamp, Michel Meunier und Stefan Nolte (Hg.): SPIE LASE. San Francisco, California, USA, Saturday 21 January 2012: SPIE (SPIE Proceedings), S. 824711.

- Lauer, Benjamin; Jaeggi, Beat; Zhang, Yiming; Neuenschwander, Beat (2015): Measurement of the maximum specific removal rate. Unexpected influence of the experimental method and the spot size. In: Laser Institute of America LIA (Hg.): ICALEO 2015, 34th International Congress on Applications of Lasers & Electro-Optics. Conference Proceedings : October 18-22, 2015. Atlanta, Ga., USA. ICALEO 2015. Atlanta, October 18-22, S. 146–154.
- Loor, Ronny de; Penning, Lars; Slagle, Rick (2014): Polygon Laser Scanning. In: *LTI* 11 (3), S. 32–34. DOI: 10.1002/latj.201400033.
- Manz AG (2015): New Technology for Laser Drilling of Ceramic Films. Greater productivity with a divided laser beam. In: *LTI* 12 (1), S. 14. DOI: 10.1002/latj.201590001.
- Neuenschwander, B.; Jaeggi, B.; Schmid, M.; Hennig, G. (2014): Surface Structuring with Ultra-short Laser Pulses. Basics, Limitations and Needs for High Throughput. In: *Physics Procedia* 56, S. 1047–1058. DOI: 10.1016/j.phpro.2014.08.017.
- Rung, Stefan (2013): Laserscribing of Thin Films Using Top-Hat Laser Beam Profiles. In: *JLMN* 8 (3), S. 309–314. DOI: 10.2961/jlmn.2013.03.0021.
- Schille, Jörg; Schneider, Lutz; Löschner, Udo (2015): Lasermikrobearbeitung mit hochrepetierenden ultrakurzpuls-Lasersystemen. In: Hochschule Mittweida, University of Applied Sciences (Hg.): Scientific Reports. Lasertechnik. 24th International Scientific Conference. Mittweida, 19.-20.11. Hochschule Mittweida, University of Applied Sciences. 6 Bände (4), S. 12–16.
- Smarra, M.; Dickmann, K. (2016): Enhancing ablation efficiency in micro structuring using a deformable mirror for beam shaping of ultra-short laser pulses. In: Udo Klotzbach, Kunihiro Washio und Craig B. Arnold (Hg.): SPIE LASE. San Francisco, California, United States, Saturday 13 February 2016: SPIE (SPIE Proceedings), S. 97360.
- Smarra, Marco; Dickmann, Klaus (2015): ULTRA-SHORT PULSE LASER BEAM SHAPING FOR MICROSTRUCTURING USING A DEFORMABLE MIRROR. In: Laser Institute of America LIA (Hg.): ICALEO 2015, 34th International Congress on Applications of Lasers & Electro-Optics. Conference Proceedings : October 18-22, 2015. Atlanta, Ga., USA. ICALEO 2015. Atlanta, October 18-22, S. 213–216.
- Smarra, Marco; Hildenhagen, Jens; Dickmann, Klaus (2015): INLINE PROCESS ANALYSIS AND CONTROL USING OPTICAL MEASUREMENT FOR THE ULTRA-SHORT PULSE LASER ABLATION OF CAD DESIGNED MICROSTRUCTURES. In: Laser Institute of America LIA (Hg.): ICALEO 2015, 34th International Congress on Applications of Lasers & Electro-Optics. Conference Proceedings : October 18-22, 2015. Atlanta, Ga., USA. ICALEO 2015. Atlanta, October 18-22, S. 172–177.